

# Ablation of Retinal Horizontal Cells from Adult Mice Leads to Rod Degeneration and Remodeling in the Outer Retina

Stephan Sonntag,<sup>1\*</sup> Karin Dedek,<sup>2\*</sup> Birthe Dorgau,<sup>2</sup> Konrad Schultz,<sup>2</sup> Karl-Friedrich Schmidt,<sup>3</sup> Kerstin Cimiotti,<sup>1</sup> Reto Weiler,<sup>2</sup> Siegrid Löwel,<sup>3</sup> Klaus Willecke,<sup>1\*</sup> and Ulrike Janssen-Bienhold<sup>2\*</sup>

<sup>1</sup>Life and Medical Sciences Institute, University of Bonn, D-53115 Bonn, Germany, <sup>2</sup>Department of Neurobiology, University of Oldenburg, D-26111 Oldenburg, Germany, and <sup>3</sup>Bernstein Focus Neurotechnology and Johann-Friedrich-Blumenbach Institut für Zoologie und Anthropologie, Georg-August-Universität Göttingen, D-37075 Göttingen, Germany

In the brain, including the retina, interneurons show an enormous structural and functional diversity. Retinal horizontal cells represent a class of interneurons that form triad synapses with photoreceptors and ON bipolar cells. At this first retinal synapse, horizontal cells modulate signal transmission from photoreceptors to bipolar cells by feedback and feedforward inhibition. To test how the fully developed retina reacts to the specific loss of horizontal cells, these interneurons were specifically ablated from adult mice using the diphtheria toxin (DT)/DT-receptor system and the *connexin57* promoter. Following ablation, the retinal network responded with extensive remodeling: rods retracted their axons from the outer plexiform layer and partially degenerated, whereas cones survived. Cone pedicles remained in the outer plexiform layer and preserved synaptic contacts with OFF but not with ON bipolar cells. Consistently, the retinal ON pathway was impaired, leading to reduced amplitudes and prolonged latencies in electroretinograms. However, ganglion cell responses showed only slight changes in time course, presumably because ON bipolar cells formed multiple ectopic synapses with photoreceptors, and visual performance, assessed with an optomotor system, was only mildly affected. Thus, the loss of an entire interneuron class can be largely compensated even by the adult retinal network.

## Introduction

The functioning of neuronal networks depends on the spatially ordered organization of projection neurons and interneurons and their synaptic connections. While projection neurons, e.g., pyramidal cells, comprise a rather homogeneous group of neurons with relatively uniform features (Flames and Marín, 2005), interneurons show an enormous structural and functional diversity in the brain, including the retina (Masland, 2001; Schilling et al., 2008). They represent important elements of neuronal networks as they are often inhibitory and balance excitation (Markram et al., 2004; Moore et al., 2010). Because of the sheer number of different interneuron classes, the response of a neuronal network to the loss of a single interneuron type is difficult to investigate; especially if one aims to study mature neuronal net-

works, it is essential to allow the network to develop normally before perturbing it (Nirenberg and Cepko, 1993). Here, we have overcome this obstacle by generating a new transgenic mutant and exclusively ablated a specific class of interneurons—the horizontal cells—from the adult mouse retina.

Mouse horizontal cells are electrically coupled by gap junctions made of connexin57 (Cx57) (Hombach et al., 2004; Shelley et al., 2006; Janssen-Bienhold et al., 2009), forming an extensive network that feeds back onto photoreceptors and feeds forward to bipolar cells. In photoreceptors, two morphologically distinct types of synaptic contacts have been characterized: flat contacts and invaginating synapses called “triads.” Flat contacts (basal junctions) are formed by OFF bipolar cell dendrites contacting the photoreceptor base (Haverkamp et al., 2000), whereas triad synapses consist of a presynaptic ribbon (the specialized glutamate release machinery of photoreceptors) and three postsynaptic elements: two lateral horizontal cell dendrites and one or two centrally oriented ON bipolar cell dendrites (Rao-Mirotnik et al., 1995). At these highly specialized synapses, signal transmission between photoreceptors and horizontal cells is reciprocal: horizontal cells receive input from photoreceptors via ionotropic glutamate receptors (GluRs) (Haverkamp et al., 2000) and feed positive (Jackman et al., 2011) and negative signals back to cones (Kamermans et al., 2001; Vessey et al., 2005) and rods (Thoreson et al., 2008), thereby regulating photoreceptor output.

Ablation of horizontal cells from the developing retina showed that horizontal cells are important for the generation of triad synapses (Messersmith and Redburn, 1990; Hammang et al., 1993). However, how the mature retina responds to the loss of

Received Jan. 31, 2012; revised May 31, 2012; accepted June 12, 2012.

Author contributions: S.S., K.D., R.W., S.L., K.W., and U.J.-B. designed research; S.S., K.D., B.D., K.S., K.-F.S., K.C., and U.J.-B. performed research; K.C. contributed unpublished reagents/analytic tools; S.S., K.D., B.D., K.S., K.-F.S., and U.J.-B. analyzed data; S.S., K.D., K.-F.S., and U.J.-B. wrote the paper.

This work was supported by Deutsche Forschungsgemeinschaft Grants W1270/31-1 and SFB 645-B2 (K.W.) and DE 1154/3-1 (K.D. and U.J.-B.) and European Commission Seventh Framework Programme RETICIRC Grant 223/56 (R.W.). We thank C. Siegmund, B. Kewitz, and S. Wallenstein for excellent technical assistance, and F. Müller (FZ Jülich, Jülich, Germany), B. Hamprecht (University of Tübingen, Germany), and S. Haverkamp (MPI for Brain Research, Frankfurt, Germany) for the generous gifts of the anti-HCN4, anti-glypho, and anti-GluR5 antibodies, respectively. We also thank J. Ammermüller for help with ERG measurements. We are grateful to J. Trümpler for critical reading of an earlier version of this manuscript.

\*S.S., K.D., K.W., and U.J.-B. contributed equally to this work.

Correspondence should be addressed to Dr. Ulrike Janssen-Bienhold, University of Oldenburg, Department of Neurobiology, P.O. Box 2503, D-26111 Oldenburg, Germany. E-mail: ulrike.janssen.bienhold@uni-oldenburg.de.

S. Sonntag's present address: PolyGene AG, CH-8153 Rümlang, Switzerland.

DOI:10.1523/JNEUROSCI.0442-12.2012

Copyright © 2012 the authors 0270-6474/12/3210713-12\$15.00/0

horizontal cells has never been investigated, as ablation was never entirely horizontal cell specific and was only induced before the retina was fully developed [for the neonatal retina, see the study by Messersmith and Redburn (1990); for retina in the first postnatal week, see the study by Hammang et al. (1993)].

Here, we introduce a new mouse model, the *Cx57+DTR* mouse line, which enables the exclusive ablation of horizontal cells from the adult mouse retina via a system of diphtheria toxin (DT) and the DT receptor (DTR) (Buch et al., 2005). Morphological and functional consequences for the retinal network were followed for more than 6 months and evaluated at three different levels: (1) on the structural and ultrastructural level, (2) on the level of retinal output, and (3) on the behavioral level.

## Materials and Methods

**Generation of *Cx57/DTR knock-in mice.*** For the ablation of retinal horizontal cells, we generated a mouse line that expresses the primate DTR as a fusion protein with enhanced green fluorescent protein (eGFP; kind gift from Dr. T. Buch, TU München, München, Germany) under the control of the endogenous promoter of *Cx57*. For this, the main part of the *Cx57* coding region in exon 2 was replaced by the coding sequence for the DTR-eGFP fusion protein via homologous recombination in mouse embryonic stem cells, analogous to the *Cx57* knock-out (KO) mouse line (Hombach et al., 2004). To generate the targeting vector pKW-DTRfrtCre, we used the *Cx57* KO vector (Hombach et al., 2004) and replaced the coding sequence of the *LacZ* cDNA, inserted into exon 2 of *Cx57*, with the frt-flanked coding sequence of *DTR-eGFP* followed by the coding sequence of *Cre recombinase*. In addition to the *Cx57* promoter-dependent expression of the DTR, this allows flippase (FLP)-mediated excision of *DTR-eGFP*, leaving the *Cre recombinase* under the control of the *Cx57* promoter. For selection of embryonic stem cells, a neomycin resistance gene under the control of the phosphoglycerate kinase promoter (*PGK-neo*) was inserted into intron 2 of *Cx57* (Fig. 1A).

Transfection of embryonic stem cells, screening for recombined ES-cell clones and blastocyst injection were performed as described previously (Theis et al., 2000). Briefly, HM-1 ES cells (Magin et al., 1992) were transfected via electroporation with the targeting vector pKW-DTRfrtCre linearized with AhdI. After 10 d of selection with 350  $\mu\text{g}/\text{ml}$  G418 (*O*-2-Amino-2,7-dideoxy-D-glycero- $\alpha$ -D-glucopyranosyl-(1 $\rightarrow$ 4)-*O*-(3-deoxy-4-C-methyl-3-(methylamino)- $\beta$ -L-arabinopyranosyl-(1 $\rightarrow$ 6))-D-streptomycin; Invitrogen), 200 clones were isolated, and 10 clones with correct homologous recombination on both arms were identified via PCR and confirmed by Southern blot analyses. Two clones with a correct karyotype were injected into C57BL/6 blastocysts. Male mice with a high degree of coat color chimerism were mated to C57BL/6 mice to generate heterozygous *Cx57/DTR* mice. Correct homologous recombination in heterozygous and homozygous *Cx57/DTR* mice was confirmed by Southern blot hybridization of ScaI cut genomic DNA from liver with a 3' external probe from intron 2 of *Cx57*, resulting in a 6.6 kb signal for the *Cx57* wild-type and 7.2 kb for the *Cx57/DTR* allele (Fig. 1A,B). For the present study, only heterozygous mice were used for horizontal cell ablation, since they still carry one allele of *Cx57*.

**Genotyping of *Cx57/DTR* mice.** For the genotyping of *Cx57/DTR* mice, a three-primer PCR with a common primer homologous to a part of intron 1 of *Cx57* (5'-CAATGAGTGGTAGTGGGAAGCTTAG-3') was used in combination with either a *Cx57* exon 2-specific primer (5'-GGCCCATATACACCAAAGAAGGG-3'), leading to an amplicon of 720 bp, or a *DTR*-specific primer (5'-CATTCTCCGTGGATGCAGAA GTC-3'), leading to an amplicon of 560 bp (Fig. 1A,C). The following PCR parameters were used: 94°C for 4 min; 30 cycles of 94°C for 45 s, 63°C for 1 min, and 72°C for 1 min; and a final step of 72°C for 7 min.

**DT injection.** Mice were kept in accordance to governmental and institutional care regulations and were maintained under a 12 h light/dark cycle. Adult (2–4 months) *Cx57+/+* and *Cx57+DTR* mice were injected intraperitoneally with 100 ng diphtheria toxin (Sigma) for 3 consecutive days. After 2 weeks, animals were injected for another 3 d. Time points throughout the manuscript are given with reference to the last

injection day. Thus, animals analyzed 6 months after ablation had an age between 8.5 and 10.5 months.

**Morphological analyses.** Immunohistochemistry and confocal image acquisition were performed as described previously (Janssen-Bienhold et al., 2009). Briefly, eyecups of *Cx57+/+* ( $n = 6$ ) and *Cx57+DTR* mice ( $n = 6$ ) were fixed with 2% paraformaldehyde in 0.1 M phosphate buffer (PB) for 20 min. Cryosections (15  $\mu\text{m}$ ) and whole mounts ( $n = 3$  for both genotypes) were blocked with 5% ChemiBLOCKER (Millipore) in PB containing 0.2% Triton X-100 and incubated with primary antibodies at 4°C overnight (cryosections) or for 5 d (whole mounts). Secondary antibodies diluted in blocking solution were applied at room temperature for 1 h (cryosections) or at 4°C for 2 d (whole mounts). A list of antibodies and dilution factors is given in Table 1. Specimens were examined with a Leica TCS SL confocal microscope. Unless stated otherwise, maximum projections of collapsed confocal stacks are shown.

For electron microscopy, retinæ ( $n = 3$  for both genotypes) were fixed in 2% paraformaldehyde, 2.6% glutaraldehyde, and 3% sucrose in 0.05 M PB overnight at 4°C, followed by postfixation in 1% OsO<sub>4</sub> in PB. After dehydration in a series of 30 to 100% acetone, retinæ were embedded in AGAR 100 resin (AGAR Scientific). Ultrathin sections (90 nm thick) were cut with a Reichert-Jung Ultracut E and analyzed using a Zeiss 902 electron microscope.

**Electroretinography.** Scotopic and photopic ERGs of *Cx57+/+* ( $n = 4$ –7) and *Cx57+DTR* mice ( $n = 5$ –7) were recorded and analyzed as described previously (Specht et al., 2007). Before recordings, animals were dark adapted overnight. Data analysis was performed using Chart version 5.5 (AD Instruments). Statistical analysis was performed with GraphPad Prism 5. All results were validated using two-way ANOVA. Pairwise comparisons were conducted using *post hoc* Bonferroni tests.

**Extracellular recordings of ganglion cell responses.** *Cx57+/+* ( $n = 4$ ) and *Cx57+DTR* mice ( $n = 5$ ) were dark adapted for  $\geq 3$  h before being killed. Eyes were enucleated under red illumination and retinæ isolated into oxygenated Ringer's solution containing (in mM) 110 NaCl, 2.5 KCl, 1 CaCl<sub>2</sub>, 1.6 MgCl<sub>2</sub>, and 10 D-glucose, buffered with 22 NaHCO<sub>3</sub> and 5% CO<sub>2</sub>/95% O<sub>2</sub>, pH 7.4. For recordings, the retina was positioned on a piece of 2% agarose with ganglion cells facing up. The preparation was continuously superfused with oxygenated Ringer's solution (2–3 ml/min) and maintained at 33°C. Recordings were made using the Utah 100 electrode array (Cyberkinetics) and were allowed to stabilize for  $\geq 30$  min.

**Light stimulation for multielectrode recordings.** Light stimulation was performed with a white LED light source (OSTAR Lightning; Osram), controlled by MATLAB R2009a (MathWorks) via the Data Acquisition Toolbox. Light intensities were in the mesopic and photopic regime and were varied over a range of 3.9 log units (0.02 to 171.36  $\mu\text{W}/\text{cm}^2$ , corresponding to  $-0.03$  to 3.87 log cds/m<sup>2</sup>, measured with an Ocean Optics USB4000 spectrometer), exceeding the range of 2.5–3 log units in natural environments (van Hateren, 1997). Two different sets of stimuli were used: (1) full-field stimuli with a fixed intensity (0.68  $\mu\text{W}/\text{cm}^2$ , 250 ms duration, 3,750 ms interstimulus interval), which were repeated 20 times, and (2) full-field stimuli in which the intensity successively increased over a range of 3.9 log units in 0.3 log unit intervals (500 ms duration, 3500 ms interstimulus interval). Each stimulus was presented 20 times. Before each set of stimuli, the retina was allowed to dark adapt for 5 min.

**Data processing and analysis for multielectrode recordings.** Extracellular spikes were sampled at 30 kHz, amplified, thresholded, and stored for off-line analysis using the Cerebus Data Acquisition System (Cyberkinetics). Spikes were sorted into units using the supervised *k* means clustering software SpikeSorter (Cyberkinetics). Time-stamp data for each unit were analyzed using Neuroexplorer (Nex Technologies) and self-made programs written in MATLAB. Peristimulus time histograms (PSTHs) were calculated for each unit and intensity with a bin width of 1 ms. PSTHs were smoothed with a Gaussian filter ( $\sigma = 6$  ms) to determine time to peak (time from stimulus onset or offset to the peak firing rate); variation of these parameters did not qualitatively influence the results. To classify ganglion cells, the response dominance index (RDI) was calculated from the peak firing rates during the ON ( $R_{\text{ON}}$ ) and OFF portions ( $R_{\text{OFF}}$ ) of the full-field stimulus (2.71  $\mu\text{W}/\text{cm}^2$ ) using the equation (Tian and Copenhagen, 2003)  $\text{RDI} = (R_{\text{ON}} - R_{\text{OFF}})/(R_{\text{ON}} + R_{\text{OFF}})$ .

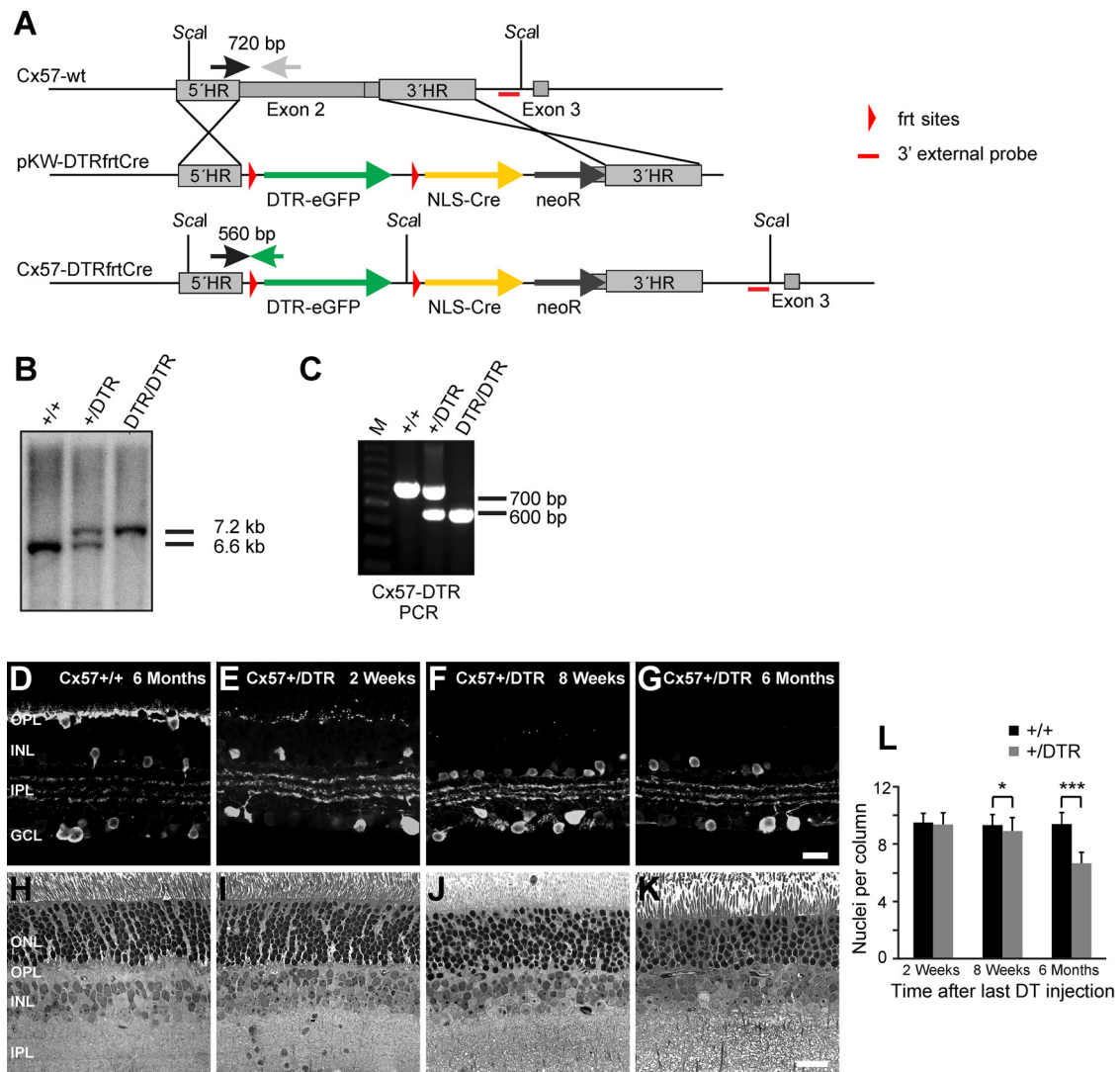


**Figure 1.** Generation of horizontal cell-deficient mice and effects of horizontal cell ablation on retina morphology. **A**, The diagram shows the homologous recombination of the *Cx57* locus with the exchange vector pKW-DTRfrtCre and the resulting *Cx57/DTR* allele. Most of exon 2 was exchanged for the coding sequence of the DTR fused with that of eGFP. This sequence was flanked by *frt* sites, the recognition sites of FLP recombinase, followed by the coding sequences of a nuclear localized Cre recombinase (NLS-Cre) and a neomycin resistance (*neoR*) cassette. Positions of primers and sizes of products for genotyping PCR, as well as restriction sites and the probe for Southern blot analyses, are indicated. **B**, Southern blot analysis with genomic DNA from *Cx57*+/+, *Cx57*+/DTR, and *Cx57DTR/DTR* mice cut with *Scal* and probed using a sequence following the 3' homology region in the *Cx57* locus (**A**). This resulted in a 6.6 kb signal for the wild-type allele and a 7.2 kb signal for the *Cx57/DTR* allele. **C**, PCR analysis of all three genotypes using the primer depicted in **A**. The wild-type allele resulted in a PCR product of 720 bp, whereas a 560 bp fragment was generated for the *Cx57/DTR* allele. **D–G**, Retinal cryosections of DT-treated *Cx57*+/+ and *Cx57*+/DTR mice were stained with anti-calbindin antibodies. *Cx57*+/DTR mice lacked calbindin-positive horizontal cells 8 weeks (**F**) and 6 months (**G**) after the last DT injection. Calbindin-positive amacrine and ganglion cells were not affected. **H–K**, Toluidine-stained semithin sections (1  $\mu$ m) of agar-embedded retinæ prepared from *Cx57*+/+ and *Cx57*+/DTR mice. Compared to the wild-type, the OPL became progressively thinner in *Cx57*+/DTR retinæ within 6 months after DT injection. The characteristic columnar organization of photoreceptor nuclei observed in *Cx57*+/+ retinæ (**H**) partially disappeared in *Cx57*+/DTR retinæ (**J, K**). Scale bars: **G** (for **D–G**), **K** (for **H–K**), 20  $\mu$ m. **L**, Quantification of photoreceptor nuclei per column in *Cx57*+/+ ( $n = 3$ ) and *Cx57*+/DTR retinæ ( $n = 3$ ). *Cx57*+/DTR retinæ contained significantly fewer nuclei per column. Values are given as mean  $\pm$  SD; a *t* test was used to compare means: \* $p < 0.05$ ; \*\*\* $p < 0.001$ .

The RDI can have values between  $-1$  and  $1$ . Ganglion cells with an RDI of  $\geq 0.33$  were defined as ON cells, those with an RDI less than or equal to  $-0.33$  were defined as OFF cells, and cells with an intermediate RDI near  $0$  were defined as ON-OFF cells.

**Determining intensity-response functions from ganglion cell responses.** To analyze the intensity range of ON ganglion cell responses in control and horizontal cell-ablated mice, we determined the mean firing rate during the first 500 ms of the light stimulus. To account for differences in firing rates, mean firing rates were normalized. Rates were plotted against the logarithm of the light intensity and fitted by a Hill equation to derive the semisaturation constant ( $I_{50}$ ) and the Hill exponent ( $K$ ). For  $I_{50}$  distributions,  $I_{50}$  values only from ON ganglion cells that had an adjusted  $R^2$  of  $\geq 0.95$  were included.

**Visual acuity and contrast sensitivity.** Visual acuity was assessed using a virtual-reality optomotor system and performed as described previously

(Goetze et al., 2010). Briefly, freely moving animals were exposed to moving sine wave gratings of various spatial frequencies and contrasts, and reflexively tracked the gratings using head movements as long as they could see the gratings. Contrast thresholds at the following six spatial frequencies were measured: 0.031, 0.064, 0.092, 0.103, 0.192, and 0.272 cycles per degree.

## Results

### Generation of *Cx57*+/DTR mice to induce horizontal cell ablation

Several studies have attempted to ablate horizontal cells from the developing mammalian retina (Messersmith and Redburn, 1990; Hammang et al., 1993; Peachey et al., 1997). However, kainic

**Table 1. Primary and secondary antibodies used in this study**

Antigen	Antiserum	Source	Dilution factor
Calbindin	Rabbit anti-calbindin	Swant	1:2000
PSD-95	Mouse anti-PSD-95	Dianova	1:5000
Calsenilin	Human recombinant calsenilin	Millipore, AB1550	1:2000
CtBP2	Mouse anti-CtBP2	BD Biosciences	1:5000
Glypho	Guinea pig anti-glycogen phosphorylase	Gift from B. Hamprecht (University of Tübingen, Tübingen, Germany)	1:500
Cone arrestin	Rabbit anti-cone arrestin	Millipore	1: 1000
PKC $\alpha$	Goat anti-PKC $\alpha$	Santa Cruz Biotechnology	1:500
G $_{\alpha c}$	Mouse anti-G $_{\alpha c}$	Chemicon	1:500
PKARII $\beta$	Mouse anti-PKARII $\beta$	BD Biosciences	1:2000
GluR1	Rabbit anti-mGluR1	Chemicon	1:250
mGluR6	Rabbit anti-mGluR6	Acris Antibodies	1:1000
HCN4	Rat anti-HCN4	Gift from F. Müller (FZ Jülich, Jülich, Germany)	1:100
CtBP2	Mouse anti-CtBP2	BD Biosciences	1:5000
Bassoon	Mouse anti-bassoon	Stressgen Bioreagents	1:10,000
S-opsin	Goat anti-S-opsin	Santa Cruz Biotechnology	1:100
Rabbit IgG	Goat anti-rabbit IgG Alexa 488	Invitrogen	1:600
	Donkey anti-rabbit IgG Alexa 488	Invitrogen	1:600
Mouse IgG	Goat anti-mouse IgG Alexa 568,	Invitrogen	1:600
	Goat anti-mouse IgG Cy3 and Cy5	Jackson ImmunoResearch	1:600
Goat IgG	Donkey anti-goat IgG Cy3 and Cy5	Jackson ImmunoResearch	1:600
Rat IgG	Goat anti-rat IgG Cy3	Dianova	1:600

acid- and oncogene-induced ablations were not horizontal cell specific, as amacrine cells were also affected (Messersmith and Redburn, 1990; Hammang et al., 1993; Peachey et al., 1997). Thus, we used a different approach based on *Cx57*, whose promoter is only active in retinal horizontal cells and in the thymus medulla (Hombach et al., 2004; Tykocinski et al., 2010). This restricted expression makes the *Cx57* promoter ideally suited for cell type-specific ablation. This was achieved using the toxin of the *Corynebacterium diphtheriae* (DT) and its receptor (DTR). We generated a transgenic mouse line via homologous recombination in mouse embryonic stem cells in which most of exon 2 of *Cx57* (Hombach et al., 2004) was replaced by the coding sequence for the primate *DTR* (Buch et al., 2005) (Fig. 1).

#### Time course of horizontal cell ablation

To study effects on the adult retinal network, horizontal cell ablation was induced by DT injection only after the retina was fully developed. Adult mice were injected intraperitoneally with 100 ng DT for 3 d followed by three additional doses 2 weeks later. This approach resulted in complete and exclusive ablation of horizontal cells within 8 weeks of the last injection.

Loss of horizontal cells was monitored using calbindin immunoreactivity, as calbindin is a marker for horizontal cells in the mouse retina (Haverkamp and Wässle, 2000) (Fig. 1D). Two weeks after the last DT injection, somatic calbindin immunoreactivity was no longer detectable in *Cx57+DTR* mice (Fig. 1E). Consistently, >99% of horizontal cell *LacZ* signals were lost (data not shown). At this time point, only small calbindin-positive puncta remained in the distal outer plexiform layer (OPL) (Fig. 1E), but they were absent in retinæ of *Cx57+DTR* mice 8 weeks (Fig. 1F) and 6 months (Fig. 1G) after the last DT injection, indicating that horizontal cell ablation was complete after 8 weeks. In contrast, calbindin-immunoreactive amacrine and ganglion cells were not affected by DT treatment in *Cx57+DTR* mice (Fig. 1E–G), demonstrating the specificity of ablation.

#### Horizontal cell ablation led to a thinning of the OPL and a loss of rods

To analyze the effect of horizontal cell ablation on the structural level, we examined series of toluidine-stained semithin sections of retinæ from DT-treated wild-type and *Cx57+DTR* mice between 2 weeks and 6 months after the last DT injection (Fig. 1H–K). We found two major effects in the outer retina: (1) two weeks after DT treatment, the OPL of *Cx57+DTR* retinæ appeared to be thinner (Fig. 1I). Also, thinning was progressive: the OPL almost completely disappeared by 6 months after ablation (Fig. 1K). (2) Eight weeks (Fig. 1J) and 6 months (Fig. 1K) after DT treatment, the columnar alignment of photoreceptor nuclei was disrupted, and the number of nuclei per column was significantly smaller in treated *Cx57+DTR* mice, which lost approximately one-third of all photoreceptor nuclei in each column (Fig. 1L).

#### Horizontal cell ablation affected rods more than cones

To investigate these structural changes in greater detail, we analyzed single ultrathin sections of retinæ from *Cx57+/+* and *Cx57+DTR* mice at two time points: (1) 8 weeks (data not shown), when ablation was just complete, and (2) 6 months after the last toxin injection (Fig. 2), to assess long-term effects on the retinal network.

Eight weeks (data not shown) and 6 months (Fig. 2) after DT treatment, the OPL of *Cx57+DTR* retinæ appeared thinner than in the wild-types (Fig. 2A,B), consistent with our light microscopical findings. In wild-type retinæ, electron microscopy showed numerous rod spherules with single ribbon synapses and mitochondria in the distal OPL. Horizontal cell processes and rod bipolar cell dendrites formed the typical triad configuration (data not shown). Cone pedicles were identified less frequently, but always contained multiple ribbons (Fig. 2C). In cone pedicles of *Cx57+DTR* mice, synaptic ribbons were still present but shorter than in control retinæ (Fig. 2D, arrowheads). Invaginating post-

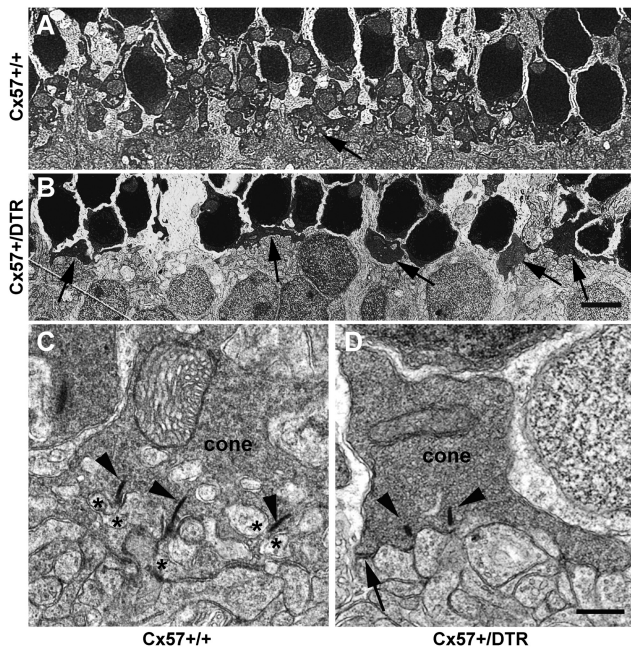


**Figure 2.** Horizontal cell ablation caused a thinning of the outer plexiform layer. **A–D**, Electron microscopic analysis of *Cx57*<sup>+/+</sup> (**A**, **C**) and *Cx57*<sup>+/DTR</sup> retinas (**B**, **D**) 6 months past DT treatment. **A**, **B**, Low-magnification montage of the OPL of *Cx57*<sup>+/+</sup> (**A**) and *Cx57*<sup>+/DTR</sup> retinas (**B**). In the OPL of control mice, numerous cross-sectioned rod spherules were localized at the distal border, adjacent to the outer nuclear layer. A cone pedicle present among the spherules is marked by an arrow. The proximal OPL showed a dense network of intermingling dendrites of horizontal and bipolar cells (**A**). In contrast, the OPL of the horizontal cell-ablated retina almost disappeared. Rod spherules, if present at all, appeared rudimentary; cone pedicles appeared smaller and flattened (black arrows). Also, the number of processes was highly reduced, and fine, intermingling dendrites were primarily found at the base of the remaining cone pedicles (**B**). **C**, **D**, Individual cones of *Cx57*<sup>+/+</sup> (**C**) and *Cx57*<sup>+/DTR</sup> mice (**D**). While individual cones of control mice (**C**) showed multiple invaginations (asterisks) beside ribbons (arrowheads), invaginations were lost in cones from *Cx57*<sup>+/DTR</sup> mice. Also, ribbons were shorter (**D**) than in control mice (**C**). However, flat contacts between bipolar cells and cones were preserved in horizontal cell-ablated mice (**D**, long arrow). Scale bars: (in **B**) **A**, **B**, 5  $\mu\text{m}$ ; (in **D**) **C**, **D**, 0.5  $\mu\text{m}$ .

synaptic processes were completely lost in *Cx57*<sup>+/DTR</sup> mice; however, bipolar cell dendrites formed flat contacts at cone pedicle bases (Fig. 2*B*, arrows).

To verify that lost photoreceptors (Fig. 1*L*) comprised mostly rods, we counted cone somata in whole mounts of wild-type ( $n = 3$ ) and *Cx57*<sup>+/DTR</sup> retinas ( $n = 3$ ) 6 months after DT treatment (Fig. 3). Cones were stained with antibodies against cone arrestin, and images ( $n = 6$ ) were taken from the central retina (Fig. 3*G*,*K*). The number of cone somata did not differ between wild-type ( $140 \pm 12$  per  $100 \mu\text{m}^2$ ; mean  $\pm$  SD) and *Cx57*<sup>+/DTR</sup> retinas ( $144 \pm 8$  per  $100 \mu\text{m}^2$ ). However, the shape and arrangement of cone pedicles changed. In wild-type retinas, cone pedicles were evenly distributed in the OPL with multiple diverging telodendria (Fig. 3*H*). In contrast, cone pedicles in *Cx57*<sup>+/DTR</sup> retinas showed atrophy and formed complex clusters (Fig. 3*L*, arrows). Thus, 6 months after DT treatment, the *Cx57*<sup>+/DTR</sup> retinal network comprised the same number of cones but lost the normal cone pedicle mosaic and rod photoreceptors.

To assess the changes in photoreceptor terminals, we stained retinas for PSD-95, a marker for rod and cone terminals (Koulen et al., 1998), and glycogen phosphorylase (glypho), a marker for cones and bipolar cells (Pfeiffer-Guglielmi et al., 2003), enabling us to distinguish between photoreceptor types (Fig. 3*A*,*D*). Again, the cone terminal mosaic appeared irregular in ablated retinas (Fig. 3*D*). Remaining rod spherules were occasionally

found to cluster around cone pedicles; the majority of spherules, however, were located just below the outer limiting membrane (OLM) (Fig. 3*D*). These findings confirm that rod photoreceptors largely retracted their terminals in response to horizontal cell ablation, whereas cone pedicles formed clusters.

#### Contacts between cones and OFF bipolar cells were retained

To check the integrity of synaptic contacts between cone photoreceptors and OFF cone bipolar cells, we performed double-labeling experiments using antibodies against glypho and AMPA receptor subunit 1 (GluR1). In wild-type retinas, GluR1 immunoreactivity formed band-like clusters below cone pedicles (Fig. 3*B*,*C*), indicating flat contacts to OFF bipolar cells (Hack et al., 2001). In *Cx57*<sup>+/DTR</sup> retinas, distribution of GluR1 immunoreactivity was less regular, though still associated with clusters of glypho-labeled cone pedicles (Fig. 3*E*,*F*), suggesting that signal transmission between cone photoreceptors and OFF bipolar cells may still function in *Cx57*<sup>+/DTR</sup> retinas.

Since type 3a, 3b, and 4 OFF bipolar cell types contact not only cones but also rods (Mataruga et al., 2007; Haverkamp et al., 2008), we stained retinas for these three bipolar cell types. In control retinas, staining for HCN4, a marker for type 3a OFF bipolar cells (Mataruga et al., 2007), revealed that dendrites of type 3a cells surround cone pedicles like nests (Wässle et al., 2009) (Fig. 3*I*,*J*). In horizontal cell-ablated retinas, cone pedicle clusters were also encircled by type 3a dendrites. Thus, these OFF bipolar cells presumably preserved their flat contacts with cone pedicles (Fig. 3*I*–*N*, arrowheads) and also preserved dendrites in the distal OPL, possibly forming a supporting base for clustered cone pedicles (Fig. 3*N*, arrows). Rarely, we observed sprouting HCN4-positive dendrites, likely searching for rod contacts. In contrast, staining for type 3b and type 4 OFF bipolar cells using anti-protein kinase A regulatory subunit II $\beta$  (anti-PKARII $\beta$ ; Mataruga et al., 2007) and anti-calsenilin antibodies as markers (Haverkamp et al., 2008), respectively, showed that type 3b and 4 bipolar cells sent numerous sprouting dendrites into the outer nuclear layer (ONL) of horizontal cell-ablated retinas (Fig. 4*A*,*B*,*F*,*G*).

Thus, within the retinal network, OFF bipolar cells react in a cell type-specific way to horizontal cell ablation. Whereas type 3b and 4 cells showed considerable dendritic sprouting, presumably searching for rod input, type 3a dendrites largely preserved their contacts to cones.

#### Horizontal cell ablation led to formation of ectopic synapses

To assess the effect on ON bipolar cell morphology, we used markers for either rod and ON cone bipolar cells ( $G_{0\alpha}$ ) or rod bipolar cells only (PKC $\alpha$ ) (Haverkamp and Wässle, 2000). In toxin-treated wild-type retinas, the dendritic endings of labeled bipolar cells terminated in the OPL (Fig. 4*C*–*E*). In comparison, in *Cx57*<sup>+/DTR</sup> retinas, the fine dendritic processes of invaginating (ON) bipolar cells were lost; instead, ON bipolar cells sent dendrites up to the OLM (Fig. 4*H*,*I*). As all ectopic  $G_{0\alpha}$ -labeled dendrites in the ONL were also positive for the rod bipolar cell marker PKC $\alpha$  (Fig. 4*J*), these data indicate that only rod bipolar cells extended their dendrites into the ONL.

We next analyzed *Cx57*<sup>+/DTR</sup> retinas for the presence of ectopic synapses, i.e., displaced synaptic contacts between second-order neurons and photoreceptors (Peng et al., 2003; Cuenca et al., 2004; Strettoi et al., 2004; Marc et al., 2007). Interestingly, in mutants for the ribbon synaptic protein bassoon, ON bipolar cell dendrites sprout along horizontal cell dendrites extending into the ONL (Specht et al., 2007). Thus, we tested for ectopic

synapses in horizontal cell-ablated retinæ and stained retinæ for PKC $\alpha$  and PSD-95 (Fig. 5*A,B,E,F*), as well as PKC $\alpha$ , CtBP2, and the metabotropic GluR6 (mGluR6; Fig. 5*C,D,G,H*), which is located at ON bipolar cell dendrites (Masu et al., 1995). Six months past DT treatment, PSD-95 immunosignals were strongly reduced in the OPL of *Cx57+/-DTR* retinæ compared to control retinæ. Retracted photoreceptor terminals colocalized with sprouted PKC $\alpha$ -positive dendrites in the ONL (Fig. 5*E,F*, arrowheads). Consistently, CtBP2-labeled ribbons and postsynaptic mGluR6 immunosignals (Fig. 5*G,H*) were scattered across the ONL. Individual PKC $\alpha$ -positive dendrites were decorated with mGluR6-positive puncta in close association to CtBP2-positive synaptic ribbons (Fig. 5*G,H*), indicating that rod ON bipolar cell dendrites reached ectopic glutamate release sites even without horizontal cell dendrites guiding them.

Electron microscopy verified these findings: 6 months after horizontal cell ablation, ectopic ribbons were found in the central to distal ONL (Fig. 5*I–K*). Ribbons were observed in rod somata and were covered with vesicles. As bipolar cell dendrites contacted these structures (Fig. 5*J*), it seems safe to assume that ectopic ribbons covered with vesicles may in fact represent ectopic synapses. Consistent with our light microscopic findings, ectopic synaptic ribbons (Fig. 5*K*, long arrow) were also found close to the OLM (Fig. 5*K*, short arrows).

To test whether ectopic synapses may also represent ectopic OFF bipolar cell contacts, we stained wild-type and *Cx57+/-DTR* retinæ with antibodies against the ionotropic glutamate receptor subunits GluR1 and GluR5 and the marker for type 3b OFF bipolar cells, PKARII $\beta$ . However, only occasionally we found GluR1 and GluR5 expressed on type 3b dendrites in the ONL (data not shown), suggesting that ectopic synapses of OFF bipolar cells are only sporadic.

Marc et al. (2007) and Jones et al. (2011) reported that rod ON bipolar cells may switch their glutamate receptor expression from mGluR6 to ionotropic glutamate receptors when contacting cones in degenerate (rodless) retinæ, presumably because the glutamate concentration at flat contacts between cones and rod bipolar cells is low and induces the expression of a higher-affinity glutamate receptor (Marc et al., 2007; Jones et al., 2011). To test whether ON bipolar cells alter their glutamate receptor expression after horizontal cell ablation, we stained for G $\alpha_{\text{Ox}}$  (ON bipolar cell marker) and GluR1 and GluR5, respectively. However, sprouted ON bipolar cell dendrites were only very rarely decorated with GluR1- or GluR5-positive puncta (data not shown). Together with our stainings for mGluR6 (Fig. 5), these data suggest that horizontal cell ablation does not induce a substantial alteration in glutamate handling in ON bipolar cells.

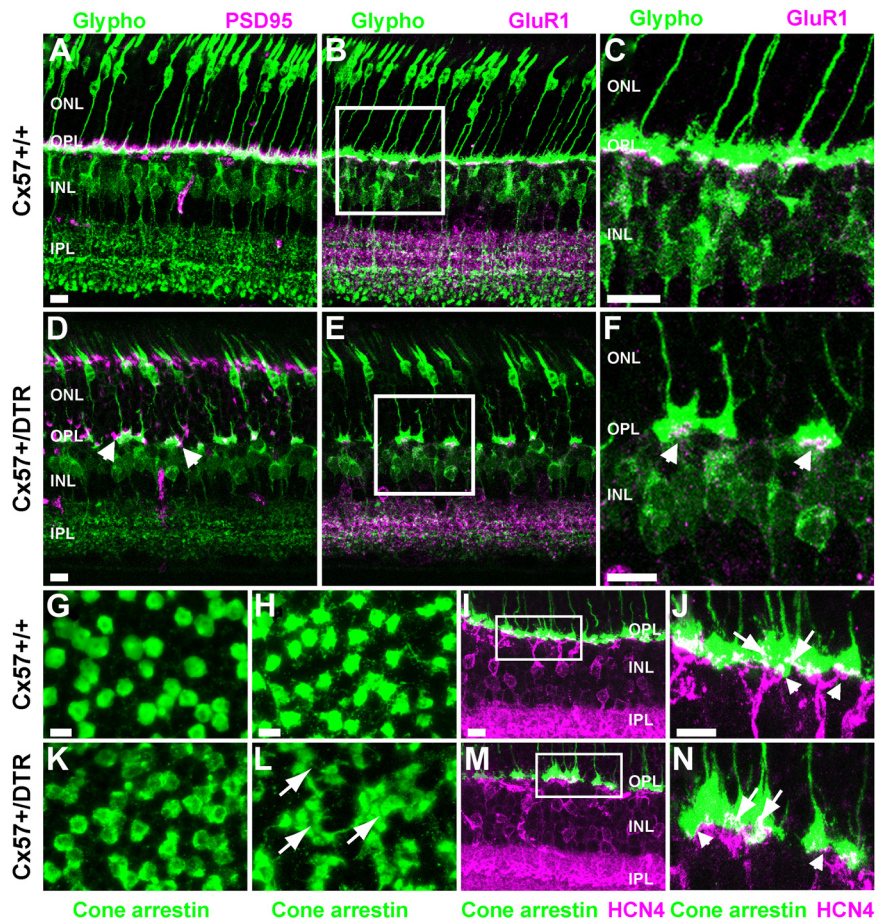


**Figure 3.** Long-term effects of horizontal cell ablation on photoreceptors 6 months after DT treatment. *A, D*, While photoreceptor endings marked with PSD-95 (magenta) were located within the OPL in control retinæ (*A*), horizontal cell ablation led to retraction of most PSD-95-positive endings in *Cx57+/-DTR* retinæ (*D*). Rod endings remaining in the OPL were associated with glycogen phosphorylase-positive cone pedicles (green, arrows). *B, C, E, F*, In treated controls, glyco-phosphorylase-positive cone pedicles (green) were associated with GluR1-positive structures in flat contacts (*B, C*). This association was preserved in horizontal cell-ablated retinæ (*E, F*). *G, H, K, L*, Retinal whole mounts were stained for cone arrestin (green), and confocal images were taken from the distal ONL (*G, K*) and the pedicle area of the OPL (*H, L*) of *Cx57+/-* (*G, H*) and *Cx57+/-DTR* retinæ (*K, L*) to control for signs of degeneration in cones. In contrast to the typical cone mosaic found in the wild-types (*G, H*), *Cx57+/-DTR* retinæ showed abnormal clusters of cone pedicles (*L*, arrows). *I, J, M, N*, Double-staining for cone arrestin (green) and HCN4 (magenta), a marker for type 3a OFF bipolar cells, showed that cone pedicle clusters appear to be encircled by type 3a OFF bipolar cells (*I, M*), which preserve their flat contacts with cone pedicles (*J, N*, arrowheads) and whose dendrites appear to form a supporting base for the clustered pedicles (*J, N*, arrows). Scale bars: *A* (for *A, B*), *D* (for *D, E*), *C, F, I* (for *I, M*), *J* (for *J, N*), 10  $\mu\text{m}$ ; *G* (for *G, K*), *H* (for *H, L*), 5  $\mu\text{m}$ .

Thus, structurally, the retinal network reacts to horizontal cell loss by remodeling the outer retina, presumably forming ectopic synapses to compensate for lost contacts between ON bipolar cells and rod photoreceptors.

### Electroretinograms were impaired in horizontal cell-ablated retinæ

In many respects, the structural changes in horizontal cell-ablated retinæ resembled effects caused by the loss of synaptic proteins in photoreceptors, such as bassoon (Specht et al., 2007), CaBP4 (Haeseleer et al., 2004), and Ca $\nu$ 1.4 (Chang et al., 2006): thinning of the OPL, outgrowth of bipolar cell dendrites, and formation of putative ectopic synapses. Since mice lacking the *bassoon*, *CaBP4*, or *Cacna1f* genes showed altered ERGs (Haeseleer et al., 2004; Chang et al., 2006; Specht et al., 2007), we compared the a- and b-waves of DT-treated *Cx57+/-* and *Cx57+/-DTR* mice. Under scotopic conditions, 8 weeks after toxin injection, a-waves were not significantly different (data not

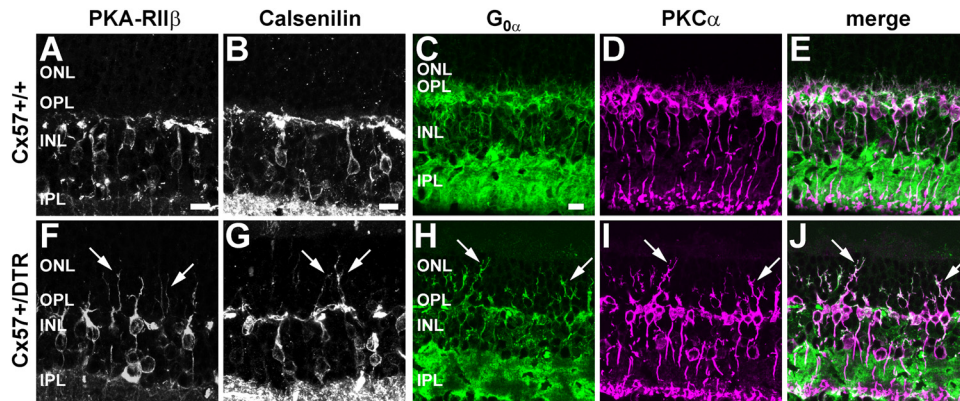


**Figure 4.** Long-term effects of horizontal cell ablation on OFF and ON bipolar cells 6 months after DT treatment. *A, B, F, G*, Type 3a OFF bipolar cells, stained with PKARIIβ-specific antibodies (*A, F*), and type 4 OFF bipolar cells, stained for calsenilin (*B, G*), developed strong extensions into the ONL after loss of horizontal cells (*F, G*). *C–E, H–J*, ON bipolar cells were double labeled with  $G_{0\alpha}$ -specific (*C, H*) and PKCα-specific antibodies (*D, I*) and showed massive protrusions of dendrites into the ONL reaching up to the OLM in horizontal cell-ablated retinæ. As all  $G_{0\alpha}$ -labeled dendrites in the ONL were also positive for the rod bipolar cell marker PKCα (*J*), we concluded that only rod bipolar cell dendrites extend into the ONL. Scale bars: *A* (for *A, F*), *B* (for *B, G*), *C* (for *C–E, H–J*), 10 μm.

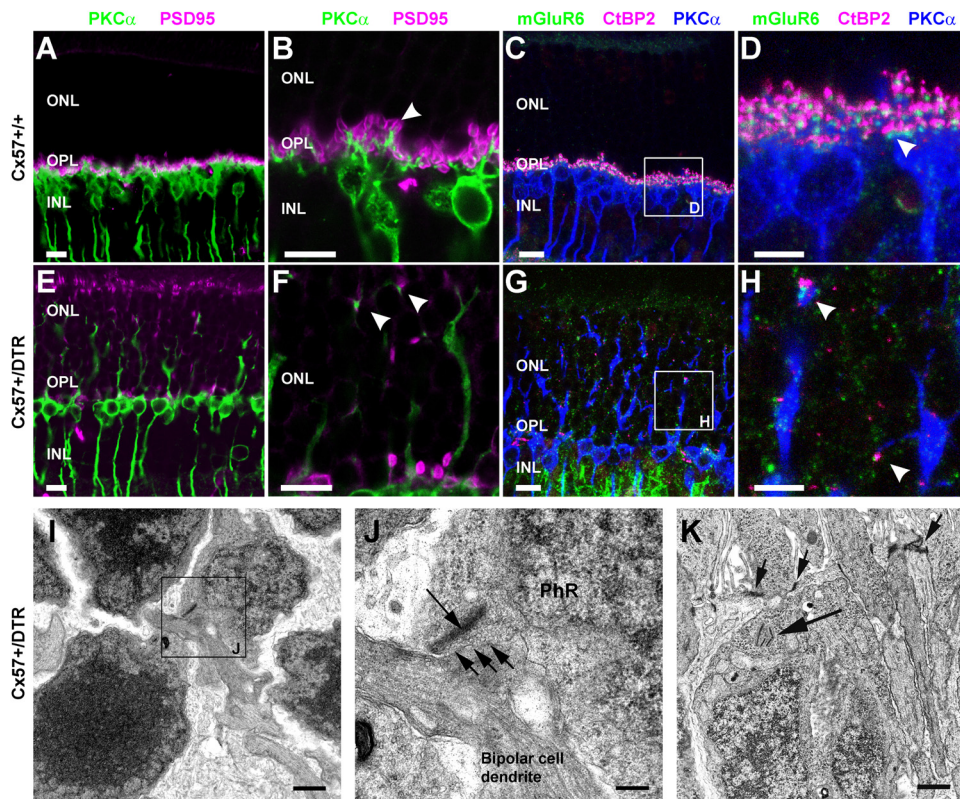


**Figure 5.** Ectopic synapses in retinæ of horizontal cell-ablated mice. *A, B, E, F*, In treated control retinæ, PKCα-positive dendrites of rod bipolar cells (green) terminated within the PSD-95-labeled rod spherules in the OPL (magenta; *B*, arrowhead). In *Cx57+/DTR* retinæ, extending bipolar cell dendrites occasionally contacted retracting PSD-95-positive rod spherules in the ONL (*F*, arrowheads). *C, D, G, H*, Triple staining with antibodies against PKCα for rod bipolar cells (blue), CtBP2 for synaptic ribbons (magenta), and mGluR6 (green), the glutamate receptor subunit of ON bipolar cells. In controls, ribbons were always closely associated with mGluR6-positive tips on rod bipolar cell dendrites (*D*, arrowhead). In *Cx57+/DTR* retinæ, the typical horseshoe-shaped structure of the ribbons was lost, but CtBP2 immunosignals were still present within the ONL and OPL. Also, in the ONL, we found sprouting dendrites decorated with mGluR6 puncta in close vicinity to CtBP2-positive ribbons (*H*, arrowheads). These structures were presumably ectopic synapses. *I, J*, A putative ectopic synapse in the ONL of a *Cx57+/DTR* retina 6 months after DT treatment. A bipolar cell dendrite contacted a vesicle-filled photoreceptor terminal (shorter arrows), in which a single synaptic ribbon is visible (long arrow). *K*, Horizontal cell-ablated mice showed ectopic ribbons surrounded by vesicles (long arrow) also close to the outer limiting membrane (short arrows). Scale bars: *A–C, E–G*, 10 μm; *D, H, 5 μm*; *I, K*, 1 μm; *J*, 250 nm.

shown). However, 6 months after DT injection, *Cx57+/DTR* mice showed significantly smaller a-wave amplitudes for intensities >0.5 cds/m<sup>2</sup> (Fig. 6*A, B*). The smaller a-wave may reflect the loss of rods in horizontal cell-ablated retinæ at this age. Also, b-wave amplitudes were significantly reduced in *Cx57+/DTR* mice for intensities >0.005 cds/m<sup>2</sup> (Fig. 6*A, B*). Moreover, the

b-wave implicit time did not change with light intensity and was longer than in controls (Fig. 6*C*).

Photopic ERGs showed basically the same effects: the b-wave amplitude of *Cx57+/+* mice increased with increasing light intensities, whereas the b-wave amplitude of *Cx57+/DTR* mice did not (Fig. 6*D*). The b-wave was significantly reduced and implicit

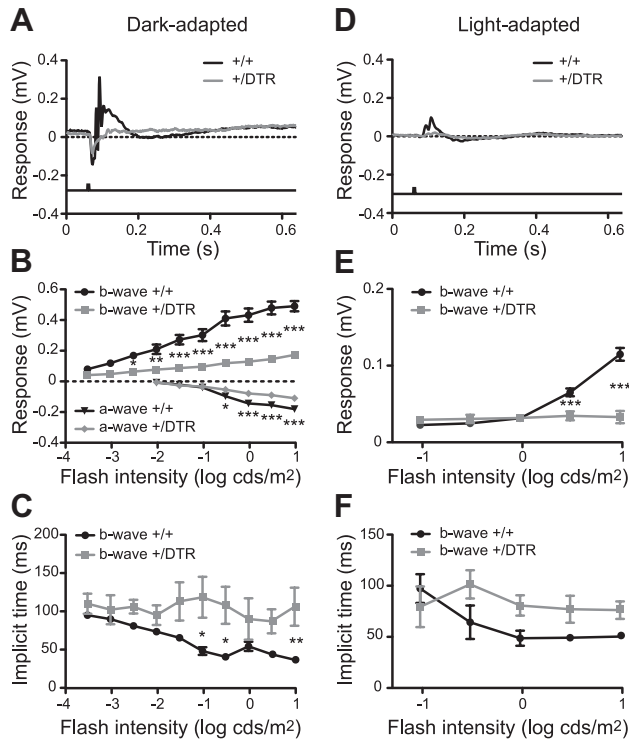


**Figure 6.** Electrophysiological responses were altered in *Cx57*<sup>+/DTR</sup> mice. **A**, Mean dark-adapted ERG responses of *Cx57*<sup>+/+</sup> ( $n = 7$ ) and *Cx57*<sup>+/DTR</sup> ( $n = 7$ ) mice at the light intensity 9.5  $\text{cds/m}^2$  6 months after DT treatment. **B**, Scotopic intensity response curves for a- and b-waves of *Cx57*<sup>+/+</sup> and *Cx57*<sup>+/DTR</sup> mice. Differences between genotypes were statistically significant (two-way ANOVA for repeated measurements, a-wave, genotype,  $p < 0.001$ ; intensity,  $p < 0.001$ ; interaction,  $p < 0.001$ ; b-wave, genotype,  $p < 0.001$ ; intensity,  $p < 0.001$ ; interaction,  $p < 0.001$ ). **C**, Implicit times of b-waves in *Cx57*<sup>+/+</sup> and *Cx57*<sup>+/DTR</sup> mice. In contrast to control mice, the b-wave implicit time of *Cx57*<sup>+/DTR</sup> mice did not change with intensity. Also, it was slower (two-way ANOVA, genotype,  $p < 0.001$ ; intensity,  $p = 0.13$ ; factor interaction,  $p = 0.31$ ). **D**, Mean light-adapted ERG responses of control and mutant mice at the light intensity 9.5  $\text{cds/m}^2$ . **E**, Photopic intensity response curves for the b-wave of *Cx57*<sup>+/+</sup> and *Cx57*<sup>+/DTR</sup> mice. At higher light intensities, *Cx57*<sup>+/DTR</sup> mice showed significantly smaller b-wave amplitudes than controls (two-way ANOVA, genotype,  $p < 0.001$ ; intensity,  $p < 0.001$ ; factor interaction  $p < 0.001$ ). **F**, Implicit time as a function of light intensity for the b-wave for *Cx57*<sup>+/+</sup> and *Cx57*<sup>+/DTR</sup> mice. Responses from *Cx57*<sup>+/DTR</sup> mice were significantly different from responses from controls (two-way ANOVA, genotype,  $p < 0.01$ ; intensity,  $p = 0.10$ ; factor interaction,  $p = 0.16$ ). Values are given as mean  $\pm$  SEM. \* $p < 0.05$ ; \*\* $p < 0.01$ ; \*\*\* $p < 0.001$  (two-way ANOVA for repeated measurements with Bonferroni *post hoc* test).

time was longer in *Cx57*<sup>+/DTR</sup> mice (Fig. 6E,F). Thus, the ERG deficits observed in horizontal cell-ablated mice were similar to those in other “no-b-wave” mutants (McCall and Gregg, 2008), i.e., mice deficient in presynaptic photoreceptor proteins (Haeleer et al., 2004; Chang et al., 2006; Specht et al., 2007) or postsynaptic proteins involved in mGluR6-mediated signaling in ON bipolar cells (Masu et al., 1995; Gregg et al., 2003).

#### ON responses were slower in horizontal cell-ablated retinae

The effects on the ERGs prompted us to analyze the output of the remaining retinal network: the ganglion cell responses. Despite the profound structural changes and deficits in the scotopic and photopic ERGs, multielectrode recordings, under mesopic/photopic conditions, showed all major physiological response types in horizontal cell-ablated retinae: transient and sustained ON responses (Fig. 7A,B), transient and sustained OFF responses (Fig. 7C,D), and ON–OFF responses (Fig. 7E,F). However, for ON ganglion cells, time to peak, measured as the time from stim-

ulus onset or offset to the peak firing rate in smoothed PSTHs ( $\sigma = 6$  ms), was significantly longer in treated retinae. This effect was statistically significant for low and high light intensities (Fig. 7G). The same effect was also observed for the ON responses of ON–OFF ganglion cells (Fig. 7K), but not for their OFF responses (Fig. 7L). Also, in OFF ganglion cells, time to peak did not differ significantly between genotypes (Fig. 7J). However, as the number of OFF ganglion cells was rather low, temporal response differences may have been obscured by cell-to-cell differences. Also, pooling data from different ganglion cell types may have masked specific changes in individual ganglion cell types.

As differences in ON cells were most prominent, we examined whether the intensity range over which ON responses could be elicited was also changed and determined intensity response functions. From these we derived the light intensity at which the response was half-maximal ( $I_{50}$ ). We did not find a significant difference between the distributions of half-maximal intensities for all ON cells from *Cx57*<sup>+/+</sup> and *Cx57*<sup>+/DTR</sup> retinae (Fig. 7H,I); the means of the distributions, however, were significantly different (Fig. 7H,I, dotted line), suggesting that a slightly higher light intensity (factor  $\sim 1.3$ ) was necessary to evoke the half-maximal response in ON cells from *Cx57*<sup>+/DTR</sup> retinae.

Thus, our data suggest that, 6 months after horizontal cell ablation, ganglion cell responses were only mildly affected. While OFF responses showed no significant differences, ON responses were slightly slower in ablated retinae.

#### Visual performance was slightly altered after horizontal cell ablation

In multielectrode recordings, only ganglion cells that showed a robust light response were assessed. Thus, we may have underestimated the effect on ganglion cell responses because severely impaired ganglion cells may have been missed. Consequently, we aimed to test the function of the retinal network on the behavioral level. Visual performance was measured as visual acuity and contrast sensitivity using a virtual-reality optomotor system (Prusky et al., 2004). Six months after DT treatment, *Cx57*<sup>+/DTR</sup> mice were able to robustly follow a visual cue. However, visual acuity was slightly lower ( $0.314 \pm 0.008$  cycles per degree; mean  $\pm$  SEM) than for *Cx57*<sup>+/+</sup> mice ( $0.374 \pm 0.0015$  cycles per degree;  $t$  test,  $p < 0.001$ ; Fig. 8A). Contrast sensitivity curves peaked at a spatial frequency of 0.064 cycles per degree for both *Cx57*<sup>+/+</sup> and *Cx57*<sup>+/DTR</sup> mice (Fig. 8B), as described previously for *C57BL/6* mice (Prusky et al., 2004). At all spatial frequencies measured, contrast sensitivity was significantly lower in horizontal cell-ablated mice than in control mice ( $t$  test,  $p < 0.01$  for all comparisons; Fig. 8B). However, this reduction was small compared to the strongly reduced contrast sensitivity in mice lacking *basoon* (Goetze et al., 2010), confirming, in line with our multielectrode recordings, that retinal processing is only subtly altered in horizontal cell-deficient mice.

Together, our anatomical, electrophysiological, and behavioral results show that horizontal cell ablation from the mature retina leads to severe changes in the outer retina: loss of synaptic contacts and restructuring of the cone pedicle mosaic in the OPL, degeneration of rod photoreceptors, and formation of ectopic synapses in the ONL. However, though ERGs are significantly impaired, ganglion cell responses and visual performance are only slightly perturbed.

#### Discussion

This study aimed to investigate the capacity of the adult retina for morphological and functional plasticity. To this end, we exclusively

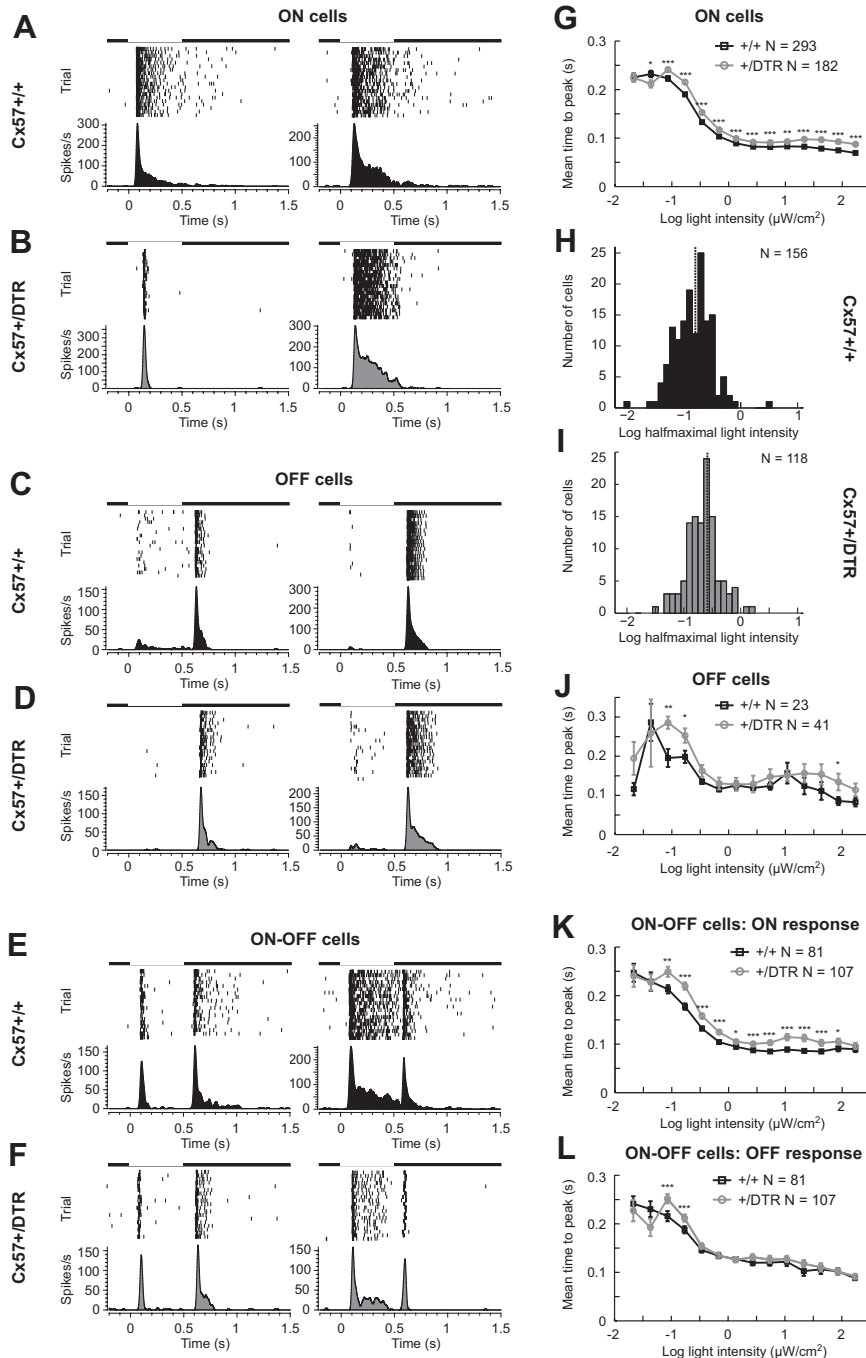


**Figure 7.** Responses to light onset were slower in *Cx57*+/*DTR* mice than in control mice. **A–F**, Representative light responses (500 ms, 0.68 μW/m<sup>2</sup>) of ON (**A, B**), OFF (**C, D**), and ON–OFF ganglion cells (**E, F**) from *Cx57*+/*+* (**A, C, E**) and *Cx57*+/*DTR* mice (**B, D, F**). Raster plots show responses from 20 trials, from which PSTHs were calculated. **G, J, K, L**, Mean time to peak plotted against light intensity for all ON (**G**), OFF (**J**), and ON–OFF ganglion cells (**K, L**) measured in both genotypes. In ON ganglion cells, differences between genotypes were statistically significant (two-way ANOVA, stimulus intensity,  $p < 0.0001$ ; genotype,  $p < 0.0001$ ; factor interaction,  $p < 0.0001$ ). In OFF ganglion cells, differences between genotypes were not statistically significant (two-way ANOVA, stimulus intensity,  $p < 0.0001$ ; genotype,  $p = 0.0531$ ; factor interaction,  $p = 0.4667$ ). In ON–OFF ganglion cells, only the ON response component was significantly slower in *Cx57*+/*DTR* mice compared to controls (two-way ANOVA, stimulus intensity,  $p < 0.0001$ ; genotype,  $p < 0.0001$ ; factor interaction,  $p < 0.05$ ). In contrast, differences in the OFF response component were not significant (two-way ANOVA, stimulus intensity,  $p < 0.0001$ ; genotype,  $p = 0.5433$ ; factor interaction,  $p = 0.121$ ). **H, I**, Distribution of log  $I_{50}$  values for all ON cells from *Cx57*+/*+* (**H**) and *Cx57*+/*DTR* mice (**I**). Only cells that had an  $R^2$  value of  $\geq 0.95$  were included. The dashed lines represent the mean of each distribution. Means were significantly different (*Cx57*+/*+*,  $-0.79 \pm 0.03 \log \mu\text{W}/\text{cm}^2$ ; *Cx57*+/*DTR*,  $-0.62 \pm 0.03 \log \mu\text{W}/\text{cm}^2$ ;  $t$  test,  $p < 0.0001$ ), although the distributions were not (Kolmogorov–Smirnov test,  $p = 0.098$ ). Mean values for individual intensities were compared using  $t$  tests. Asterisks indicate significance levels: \* $p < 0.05$ ; \*\* $p < 0.01$ ; \*\*\* $p < 0.001$ . Values are given as mean  $\pm$  SEM.  $N$ , Number of cells.

ablated horizontal cells from the mature retina and analyzed the consequences on retinal circuitry and visual performance. The many plastic changes we found, such as partial degeneration of rods, retraction of rod terminals, clustering of cone terminals, and formation of functional ectopic synapses, show that even the fully developed retina can respond with structural remodeling to a severe intervention (here, the loss of a cell type). As visual performance is not strongly impaired, this is a promising capacity that could be exploited in attempts to restore vision in patients suffering from retinal degeneration.

### Triad synapse disruption is followed by different morphological changes in rods and cones

Horizontal cell ablation led to striking changes in the morphology of the outer retina of *Cx57*+/*DTR* mice from the second week on after the last DT injection, whereas inner retinal neurons (amacrine cells, ganglion cells) and their connectivity patterns were unaffected. Horizontal cell ablation disrupted triad synapses between photoreceptors, ON bipolar cells, and horizontal cells, leading to no-b-wave mutant mice (McCall and Gregg, 2008), in which the b-wave of the ERG is strongly impaired (also see below, Physiological changes in horizontal cell-ablated mice).

What causes the loss of triad synapses following horizontal cell ablation? Horizontal cells may contribute important structural or physiological elements to the synaptic complex that allow the invagination or stabilization of bipolar cell dendrites in the photoreceptor terminals, as indicated by the important role of horizontal cells during synapse formation (Messersmith and Redburn, 1990; Rich et al., 1997). As it is likely that horizontal cell lateral elements express adhesion molecules that maintain the triad architecture, loss of these proteins after horizontal cell ablation may disrupt the synapse. To date, a few glycoproteins have been identified that play structural roles in triad synapses, such as dystrophin (Pilgram et al., 2010), retinoschisin (Johnson et al., 1996), and pikachurin (Sato et al., 2008), but these proteins are synthesized by either photoreceptors or bipolar cells. However, in chick horizontal cells, N-cadherin is required for dendrite morphogenesis and subsequent synapse formation with photoreceptor cells (Tanabe et al., 2006). Whether N-cadherin also plays a role in synapse maintenance remains to be seen.

Notably, horizontal cell ablation affected rod and cone photoreceptors dif-

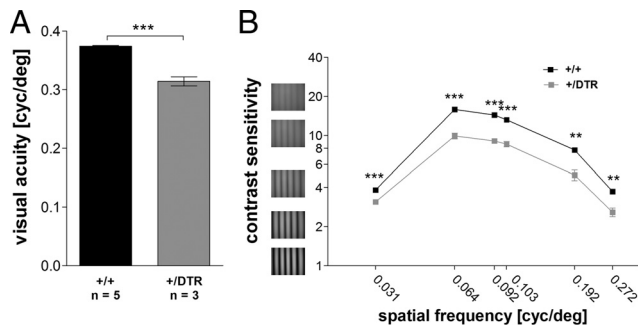


**Figure 8.** Visual performance was mildly impaired in horizontal cell-ablated *Cx57+DTR* mice. **A**, Visual acuity, measured 6 months after DT treatment, was significantly reduced in *Cx57+DTR* mice compared to wild-type controls (*Cx57+/+*; *t* test,  $***p < 0.001$ ). **B**, Contrast sensitivity was significantly reduced in *Cx57+DTR* mice at all spatial frequencies measured (*t* test,  $**p < 0.01$ ,  $***p < 0.001$ ). Values are given as mean  $\pm$  SEM.

ferently, indicating that in the mature retina, rods and cones exhibit distinct capabilities and mechanisms to cope with the loss of their synaptic contacts with horizontal cells. Almost one-third of all rod photoreceptors died within 6 months after ablation, leading to a smaller a-wave in the scotopic ERG. Most of the remaining rods retracted their terminals, and only rod spherules adjacent to cone pedicles remained in the OPL. In contrast, cones did not degenerate, but cone pedicles appeared smaller, most likely due to the loss of the many invaginations of horizontal cell and ON cone bipolar cell dendrites at triad synapses. Also, cone pedicles formed clusters in the OPL (Fig. 3*L–N*).

Though the underlying molecular mechanisms leading to the distinct responses of rods and cones to the elimination of horizontal cells from the adult retinal network are unknown, several interdependent structural or physiological mechanisms may be considered. First, as one fundamental difference between rod and cone terminals is the number of flat contacts to OFF bipolar cells, which is considerably lower for rods (Hack et al., 1999), it is possible that cones preserve their terminals in the OPL because of their more numerous OFF bipolar cell contacts. That we did not find a difference in OFF ganglion cell responses between ablated and nonablated retinæ supports the idea that connections to OFF bipolar cells are functional and may help to keep cone terminals in place in retinæ lacking horizontal cells. The distribution pattern of the remaining rod spherules in the OPL of *Cx57+/DTR* retinæ suggests that only those rod spherules survive in the OPL that are adjacent to surviving cones contacting type 3a OFF cone bipolar cells (Fig. 3*D*).

Second, neurotransmitter activity in horizontal cell-ablated retinæ may be perturbed. Glutamate is involved in excitatory neurotransmission in the outer retina, where it is tonically released from photoreceptors. Maintenance of low glutamate levels in the synaptic cleft of the triad synapse is crucial to ensure a high signal-to-noise ratio, to regulate and maintain synaptic connectivity (Gan, 2003), and to protect the neurons forming the triad from glutamate toxicity (Hasegawa et al., 2006). Since horizontal cells regulate glutamate release from photoreceptor terminals by negative and positive feedback mechanisms (Kamerms et al., 2001; Vessey et al., 2005; Jackman et al., 2011), horizontal cell ablation will inescapably perturb glutamatergic transmission between photoreceptors and the remaining bipolar cells. This will subsequently affect retinal signal transmission, and our ERG data, the recordings of ganglion cell responses, and analyses of contrast sensitivity and visual acuity corroborate this conclusion.

Since horizontal cells not only regulate glutamate release via feedback but also contribute to glutamate binding by ionotropic

glutamate receptors (Hack et al., 2001) and glutamate uptake by glutamate transporters (for review, see Barnett and Bull, 2008), lack of horizontal cells may substantially increase the glutamate concentration in the synaptic cleft. Such a rise in extracellular glutamate inhibits the glutamate/cystine antiporter (Lewerenz et al., 2012) present in photoreceptors (Hu et al., 2008), which transports cystine into and glutamate out of the cell. As cystine is required for glutathione synthesis, the major intracellular antioxidant, blockade of the antiporter will eventually lead to glutathione depletion in photoreceptors, causing oxidative damage and cell death (oxytosis) (Tan et al., 2001). Because rods and cones harbor different glutamate uptake systems with different properties (for review, see Barnett and Bull, 2008), it is likely that high extracellular glutamate concentrations affect rods and cones differently.

Thus, rods and cones may differ in their responses to horizontal cell ablation because of differences in synaptic contact number and glutamate sensitivity.

### Physiological changes in horizontal cell-ablated mice

The phenotype of horizontal cell-ablated retinæ, which lacked postsynaptic elements, matched changes induced by many presynaptic mutations in photoreceptor cells. Loss of triad synapses, a strong reduction of the ERG b-wave, and formation of ectopic synapses have been reported for mice lacking structural proteins (Specht et al., 2007), components of the voltage-dependent calcium channels (Ball et al., 2002; Chang et al., 2006), or the calcium-binding protein CaBP4 (Haeseleer et al., 2004) in photoreceptors. Thus, the retinal network responds in a similar way to two different interventions: the loss of a cell type from the fully developed retina (this study) and the lack of photoreceptor proteins, which are already missing during retina development or maturation. Interestingly, the loss of postsynaptic proteins does not induce remodeling: postsynaptic no-b-wave mutants (McCall and Gregg, 2008), such as mutants for proteins in the mGluR6-mediated signaling cascade of ON bipolar cells, show no morphological alterations in the OPL. Thus, it was hypothesized that the changes in presynaptic no-b-wave mutants are caused by changes in calcium signaling or homeostasis in presynaptic photoreceptor terminals (Bayley and Morgans, 2007). As the negative feedback from horizontal cells to cones was shown to regulate the calcium current in photoreceptors (Kamerms et al., 2001), loss of horizontal cell feedback in horizontal cell-ablated retinæ likely impairs the normal function of presynaptic calcium channels, leading to a similar phenotype as in calcium channel mutants (Ball et al., 2002; Chang et al., 2006).

As a consequence of the extensive retinal remodeling, in horizontal cell-ablated mice, effects on ganglion cell responses are subtle: ON responses show a slight loss in light sensitivity and a delay in time to peak, whereas OFF responses do not, indicating (1) that synapses between photoreceptors and OFF bipolar cells may be unimpaired and (2) that ectopic synapses between photoreceptors and ON bipolar cells may be functional but slower. This suggests that the reduction in the b-wave of the ERGs does not result from a loss of the ON pathway, but most likely originates from altered extracellular signal flow in the outer retina where circulating currents from photoreceptors (hyperpolarizing) and ON bipolar cells (depolarizing) overlap in the ONL, partially canceling each other. However, reduced and prolonged b-waves could also result when horizontal cell inhibition is switched off (Goetze et al., 2010), as is the case in our mouse model.

Despite the strong effects on electroretinograms, visual behavior was only mildly impaired in horizontal cell-ablated mice. This is in contrast to bassoon-deficient mice, in which contrast sensitivity is strongly reduced (Goetze et al., 2010), probably because glutamatergic signal transfer from photoreceptors to bipolar cells is severely diminished (Specht et al., 2007). While Goetze et al. (2010) reported for bassoon-deficient mice that ectopic synapses do not improve vision, our data suggest that ectopic synapses of ON bipolar cells contribute to the mild visual phenotype of horizontal cell-ablated mice, as ectopic synapses show the hallmarks of functional photoreceptor/bipolar cell synapses: a synaptic ribbon tethered with vesicles, presynaptic to a bipolar cell dendrite. Thus, we conclude that remodeling and ectopic synapse formation can preserve visual function even when an entire class of interneurons is ablated from the fully developed retina.

## References

- Ball SL, Powers PA, Shin HS, Morgans CW, Peachey NS, Gregg RG (2002) Role of the beta(2) subunit of voltage-dependent calcium channels in the retinal outer plexiform layer. *Invest Ophthalmol Vis Sci* 43:1595–1603.
- Barnett NL, Bull ND (2008) Glutamate transporters and retinal disease and regulation. In: *Ocular transporters in ophthalmic diseases and drug delivery* (Tombran-Tink J, Barnstable CJ, eds), pp 333–353. New York: Humana.
- Bayley PR, Morgans CW (2007) Rod bipolar cells and horizontal cells form displaced synaptic contacts with rods in the outer nuclear layer of the nob2 retina. *J Comp Neurol* 500:286–298.
- Buch T, Heppner FL, Tertilt C, Heinen TJ, Kremer M, Wunderlich FT, Jung S, Waisman A (2005) A Cre-inducible diphtheria toxin receptor mediates cell lineage ablation after toxin administration. *Nat Methods* 2:419–426.
- Chang B, Heckenlively JR, Bayley PR, Brecha NC, Davison MT, Hawes NL, Hirano AA, Hurd RE, Ikeda A, Johnson BA, McCall MA, Morgans CW, Nusinowitz S, Peachey NS, Rice DS, Vessey KA, Gregg RG (2006) The nob2 mouse, a null mutation in *Cacna1f*: anatomical and functional abnormalities in the outer retina and their consequences on ganglion cell visual responses. *Vis Neurosci* 23:11–24.
- Cuenca N, Pinilla I, Sauvé Y, Lu B, Wang S, Lund RD (2004) Regressive and reactive changes in the connectivity patterns of rod and cone pathways of P23H transgenic rat retina. *Neuroscience* 127:301–317.
- Flames N, Marin O (2005) Developmental mechanisms underlying the generation of cortical interneuron diversity. *Neuron* 46:377–381.
- Gan WB (2003) Glutamate-dependent stabilization of presynaptic terminals. *Neuron* 38:677–678.
- Goetze B, Schmidt KF, Lehmann K, Altmann WD, Gundelfinger ED, Löwel S (2010) Vision and visual cortical maps in mice with a photoreceptor synaptopathy: reduced but robust visual capabilities in the absence of synaptic ribbons. *Neuroimage* 49:1622–1631.
- Gregg RG, Mukhopadhyay S, Candille SI, Ball SL, Pardue MT, McCall MA, Peachey NS (2003) Identification of the gene and the mutation responsible for the mouse nob phenotype. *Invest Ophthalmol Vis Sci* 44:378–384.
- Hack I, Peichl L, Brandstätter JH (1999) An alternative pathway for rod signals in the rodent retina: rod photoreceptors, cone bipolar cells, and the localization of glutamate receptors. *Proc Natl Acad Sci U S A* 96:14130–14135.
- Hack I, Frech M, Dick O, Peichl L, Brandstätter JH (2001) Heterogeneous distribution of AMPA glutamate receptor subunits at the photoreceptor synapses of rodent retina. *Eur J Neurosci* 13:15–24.
- Haeseleer F, Imanishi Y, Maeda T, Possin DE, Maeda A, Lee A, Rieke F, Palczewski K (2004) Essential role of Ca<sup>2+</sup>-binding protein 4, a Cav1.4 channel regulator, in photoreceptor synaptic function. *Nat Neurosci* 7:1079–1087.
- Hammang JP, Behringer RR, Baetge EE, Palmiter RD, Brinster RL, Messing A (1993) Oncogene expression in retinal horizontal cells of transgenic mice results in a cascade of neurodegeneration. *Neuron* 10:1197–1209.
- Hasegawa J, Obara T, Tanaka K, Tachibana M (2006) High-density presynaptic transporters are required for glutamate removal from the first visual synapse. *Neuron* 50:63–74.
- Haverkamp S, Wässle H (2000) Immunocytochemical analysis of the mouse retina. *J Comp Neurol* 424:1–23.
- Haverkamp S, Grunert U, Wässle H (2000) The cone pedicle, a complex synapse in the retina. *Neuron* 27:85–95.
- Haverkamp S, Specht D, Majumdar S, Zaidi NF, Brandstätter JH, Wasco W, Wässle H, Tom Dieck S (2008) Type 4 OFF cone bipolar cells of the mouse retina express calnenilin and contact cones as well as rods. *J Comp Neurol* 507:1087–1101.
- Hombach S, Janssen-Bienhold U, Söhl G, Schubert T, Büssow H, Ott T, Weiler R, Willecke K (2004) Functional expression of connexin57 in horizontal cells of the mouse retina. *Eur J Neurosci* 19:2633–2640.
- Hu RG, Lim J, Donaldson PJ, Kalloniatis M (2008) Characterization of the cystine/glutamate transporter in the outer plexiform layer of the vertebrate retina. *Eur J Neurosci* 28:1491–1502.
- Jackman SL, Babai N, Chambers JJ, Thoreson WB, Kramer RH (2011) A positive feedback synapse from retinal horizontal cells to cone photoreceptors. *PLoS Biol* 9:e1001057.
- Janssen-Bienhold U, Trümpner J, Hilgen G, Schultz K, Müller LP, Sonntag S, Dedek K, Dirks P, Willecke K, Weiler R (2009) Connexin57 is expressed in dendro-dendritic and axo-axonal gap junctions of mouse horizontal cells and its distribution is modulated by light. *J Comp Neurol* 513:363–374.
- Johnson J, Chen TK, Rickman DW, Evans C, Brecha NC (1996) Multiple gamma-Aminobutyric acid plasma membrane transporters (GAT-1, GAT-2, GAT-3) in the rat retina. *J Comp Neurol* 375:212–224.
- Jones BW, Kondo M, Terasaki H, Watt CB, Rapp K, Anderson J, Lin Y, Shaw MV, Yang JH, Marc RE (2011) Retinal remodeling in the Tg P347L rabbit, a large-eye model of retinal degeneration. *J Comp Neurol* 519:2713–2733.
- Kamermans M, Fahrenfort I, Schultz K, Janssen-Bienhold U, Sjoerdsma T, Weiler R (2001) Hemichannel-mediated inhibition in the outer retina. *Science* 292:1178–1180.
- Koulen P, Fletcher EL, Craven SE, Brecht DS, Wässle H (1998) Immunocytochemical localization of the postsynaptic density protein PSD-95 in the mammalian retina. *J Neurosci* 18:10136–10149.
- Lewerenz J, Maher P, Methner A (2012) Regulation of xCT expression and system x (c) (-) function in neuronal cells. *Amino Acids* 42:171–179.
- Magin TM, McWhir J, Melton DW (1992) A new mouse embryonic stem cell line with good germ line contribution and gene targeting frequency. *Nucleic Acids Res* 20:3795–3796.
- Marc RE, Jones BW, Anderson JR, Kinard K, Marshak DW, Wilson JH, Wensel T, Lucas RJ (2007) Neural reprogramming in retinal degeneration. *Invest Ophthalmol Vis Sci* 48:3364–3371.
- Markram H, Toledo-Rodriguez M, Wang Y, Gupta A, Silberberg G, Wu C (2004) Interneurons of the neocortical inhibitory system. *Nat Rev Neurosci* 5:793–807.
- Masland RH (2001) Neuronal diversity in the retina. *Curr Opin Neurobiol* 11:431–436.
- Masu M, Iwakabe H, Tagawa Y, Miyoshi T, Yamashita M, Fukuda Y, Sasaki H, Hiroi K, Nakamura Y, Shigemoto R, Takada M, Nakamura K, Nakao K, Katsuki M, Nakanishi S (1995) Specific deficit of the ON response in visual transmission by targeted disruption of the mGluR6 gene. *Cell* 80:757–765.
- Mataruga A, Kremmer E, Müller F (2007) Type 3a and type 3b OFF cone bipolar cells provide for the alternative rod pathway in the mouse retina. *J Comp Neurol* 502:1123–1137.
- McCall MA, Gregg RG (2008) Comparisons of structural and functional abnormalities in mouse b-wave mutants. *J Physiol* 586:4385–4392.
- Messersmith EK, Redburn DA (1990) Kainic acid lesioning alters development of the outer plexiform layer in neonatal rabbit retina. *Int J Dev Neurosci* 8:447–461.
- Moore CI, Carlen M, Knoblich U, Cardin JA (2010) Neocortical interneurons: from diversity, strength. *Cell* 142:189–193.
- Nirenberg S, Cepko C (1993) Targeted ablation of diverse cell classes in the nervous system *in vivo*. *J Neurosci* 13:3238–3251.
- Peachey NS, Roveri L, Messing A, McCall MA (1997) Functional consequences of oncogene-induced horizontal cell degeneration in the retinas of transgenic mice. *Vis Neurosci* 14:627–632.
- Peng YW, Senda T, Hao Y, Matsuno K, Wong F (2003) Ectopic synaptogenesis during retinal degeneration in the Royal College of Surgeons rat. *Neuroscience* 119:813–820.
- Pfeiffer-Guglielmi B, Fleckenstein B, Jung G, Hamprecht B (2003) Immunocytochemical localization of glycogen phosphorylase isozymes

- in rat nervous tissues by using isozyme-specific antibodies. *J Neurochem* 85:73–81.
- Pilgram GS, Potikanond S, Baines RA, Fradkin LG, Noordermeer JN (2010) The roles of the dystrophin-associated glycoprotein complex at the synapse. *Mol Neurobiol* 41:1–21.
- Prusky GT, Alam NM, Beekman S, Douglas RM (2004) Rapid quantification of adult and developing mouse spatial vision using a virtual optomotor system. *Invest Ophthalmol Vis Sci* 45:4611–4616.
- Rao-Mirotnik R, Harkins AB, Buchsbaum G, Sterling P (1995) Mammalian rod terminal: architecture of a binary synapse. *Neuron* 14:561–569.
- Rich KA, Zhan Y, Blanks JC (1997) Migration and synaptogenesis of cone photoreceptors in the developing mouse retina. *J Comp Neurol* 388:47–63.
- Sato S, Omori Y, Katoh K, Kondo M, Kanagawa M, Miyata K, Funabiki K, Koyasu T, Kajimura N, Miyoshi T, Sawai H, Kobayashi K, Tani A, Toda T, Usukura J, Tano Y, Fujikado T, Furukawa T (2008) Pikachurin, a dystroglycan ligand, is essential for photoreceptor ribbon synapse formation. *Nat Neurosci* 11:923–931.
- Schilling K, Oberdick J, Rossi F, Baader SL (2008) Besides Purkinje cells and granule neurons: an appraisal of the cell biology of the interneurons of the cerebellar cortex. *Histochem Cell Biol* 130:601–615.
- Shelley J, Dedek K, Schubert T, Feigenspan A, Schultz K, Hombach S, Willecke K, Weiler R (2006) Horizontal cell receptive fields are reduced in connexin57-deficient mice. *Eur J Neurosci* 23:3176–3186.
- Specht D, Tom Dieck S, Ammermuller J, Regus-Leidig H, Gundelfinger ED, Brandstatter JH (2007) Structural and functional remodeling in the retina of a mouse with a photoreceptor synaptopathy: plasticity in the rod and degeneration in the cone system. *Eur J Neurosci* 26:2506–2515.
- Strettoi E, Mears AJ, Swaroop A (2004) Recruitment of the rod pathway by cones in the absence of rods. *J Neurosci* 24:7576–7582.
- Tan S, Schubert D, Maher P (2001) Oxytosis: a novel form of programmed cell death. *Curr Top Med Chem* 1:497–506.
- Tanabe K, Takahashi Y, Sato Y, Kawakami K, Takeichi M, Nakagawa S (2006) Cadherin is required for dendritic morphogenesis and synaptic terminal organization of retinal horizontal cells. *Development* 133:4085–4096.
- Theis M, Magin TM, Plum A, Willecke K (2000) General or cell type-specific deletion and replacement of connexin-coding DNA in the mouse. *Methods* 20:205–218.
- Thoreson WB, Babai N, Bartoletti TM (2008) Feedback from horizontal cells to rod photoreceptors in vertebrate retina. *J Neurosci* 28:5691–5695.
- Tian N, Copenhagen DR (2003) Visual stimulation is required for refinement of ON and OFF pathways in postnatal retina. *Neuron* 39:85–96.
- Tykocinski LO, Sinemus A, Rezavandy E, Weiland Y, Baddeley D, Cremer C, Sonntag S, Willecke K, Derbinski J, Kyewski B (2010) Epigenetic regulation of promiscuous gene expression in thymic medullary epithelial cells. *Proc Natl Acad Sci U S A* 107:19426–19431.
- van Hateren JH (1997) Processing of natural time series of intensities by the visual system of the blowfly. *Vision Res* 37:3407–3416.
- Vessey JP, Stratis AK, Daniels BA, Da Silva N, Jonz MG, Lalonde MR, Baldrige WH, Barnes S (2005) Proton-mediated feedback inhibition of presynaptic calcium channels at the cone photoreceptor synapse. *J Neurosci* 25:4108–4117.
- Wässle H, Puller C, Müller F, Haverkamp S (2009) Cone contacts, mosaics, and territories of bipolar cells in the mouse retina. *J Neurosci* 29:106–117.